Appl. Magn. Reson. 19, 141–150 (2000)

Applied Magnetic Resonance

Three-Dimensional Structure of Electron Transfer Components in Photosystem II: "2+1" ESE of Chlorophyll Z and Tyrosine D

M. Tonaka[1], A. Kawamori[1], H. Hara[2], and A. V. Astashkin[3]

[1] Faculty of Science, Kwansei Gakuin University, Japan
[2] Division of EPR Application, Bruker Japan Co. Ltd., Japan
[3] Department of Chemistry, University of Arizona, Tucson, Arizona, USA

Received December 10, 1999; revised June 15, 2000

Abstract. A "2+1" electron spin echo method has been applied to measure the orientation of the distance vector **R** from the redox-active tyrosine residue Y_D to chlorophyll Z Chl_Z in a membrane-oriented Mn-depleted preparation of photosystem II. The angle between **R** and the normal **n** to the photosystem II membranes was determined to be 50.0 ± 5° with the value of the dipolar interaction parameter D_0 = 2.0 MHz, the corresponding distance of 29.4 ± 0.5 Å, determined in a nonoriented PS II sample.

1 Introduction

In higher plants photosystem II (PS II) is composed of several intrinsic and extrinsic membrane protein complexes. Among them, the heterodimer of D1 and D2 proteins is believed to bind almost all electron transfer components of PS II. On the donor side, the primary electron donor (P680; a chlorophyll (Chl) dimer), the secondary donor Y_Z (tyrosine-161 in D1 subunit) and a cluster of four Mn atoms in the water-oxidizing complex (WOC) are included [1]. On the acceptor side, one of two pheophytin molecules accepts an electron from P680 and donates it to the primary electron acceptor plastoquinone (Q_A) wherefrom it is transferred to the secondary acceptor plastoquinone (Q_B). Besides, there are several additional redox-active components, cytochrome b_{559} (cyt b_{559}), so-called chlorophyll Z (Chl_Z; a monomer chlorophyll donor) and one more redox-active tyrosine residue Y_D (tyrosine-161 in D2 subunit) [1].

Arrays of chlorophyll (Chl) molecules constitute antenna proteins that collect and transfer light energy to the reaction center, and initiate photochemistry by electron transfer reactions. Most of Chls found in PS II are bound to light-harvesting proteins and the other Chl-binding proteins (CP43, CP47) [2–6]. In

the reaction center, there are four accessory monomer chlorophylls, of which one is designated to be Chl_Z [7].

In the normal electron transfer reaction a photo-oxidized $P680^+$ is reduced by Y_Z and then the oxidized Y_Z is reduced by the Mn cluster in WOC [8, 9]. Y_Z plays an important role as an intermediate in this reaction. Although Y_Z and Y_D are suggested to be at symmetric positions around P680, Y_D does not play a definite role in the major electron transfer reaction [10, 11]. The oxidized Y_D ($Y_D^{\bullet}$) stays usually as a very stable radical after dark adaptation. In the process of photo-inactivation, Chl_Z plays a role of intermediate in an electron transfer pathway between cyt b_{559} and $P680^+$ [1, 12]. Chl_Z is expected to be nearby to the heme of cyt b_{559} because the oxidation is very efficient, even at cryogenic temperature [12, 13]. Although the yields of photo-oxidation of cyt b_{559} and Chl_Z are low relative to those of the primary electron donors (Y_Z and WOC), these alternate electron donors can mediate a cyclic electron transfer and may play a role in protection of PS II from photo-inactivation [12, 14–18]. While the identity of the electron transfer components has been established, their geometrical arrangement inside the PS II reaction center (RC) complex has not yet been clarified owing to the difficulty of crystallization of PS II reaction center survived under X-ray analysis. Instead of X-ray analysis, the methods of the electron paramagnetic resonance (EPR) play an important role in the elucidation of the PS II structure because these electron transfer components are paramagnetic in their oxidized or reduced states.

The pulsed electron-electron double resonance (PELDOR) [19, 20] and "2+1" electron spin echo (ESE) [21, 22] methods allow one to measure directly dipole interactions between the paramagnetic centers. By applying these techniques, we have been able to improve the accuracy in estimation of the distances and in acquisition of the angular information between the redox-active components in PS II significantly [23–25, 28]. The distances from Y_D to Y_Z and to the Mn cluster in WOC have been measured to be about 29 and 27 Å, respectively [23–25]. The distance between Y_D and the species giving so-called S_3' signal in Ca^{2+}-depleted PS II was found to be about 30 Å [25].

The structural information about the electron transfer chain in PS II obtained in disordered samples is limited to the values of distances between the redox-active components. It is highly desirable, however, to clarify the three-dimensional arrangement of the electron transfer components with oriented PS II samples. One can achieve the orientation of PS II membranes on mylar sheets. The angles between the distance vectors from Y_D to Y_Z and to the Mn cluster in WOC and the membrane normals were determined to be about 100 and 110°, respectively [28]. The oriented PS II membranes were also studied to elucidate the molecular orientation of the electron carrier under investigation with respect to the membrane normal [28].

In this study we are interested in the orientation of the distance vector **R** joining the redox-active components with respect to the membrane normal in PS II. We have used the Mn-depleted PS II membranes oriented on mylar sheets to obtain the angular information of Y_D-Chl_Z distance.

2 Experimental

2.1 Samples

PS II membranes were prepared from market spinach by the method of Kuwabara and Murata [26]. Mn depletion was performed by incubating PS II membranes on ice under room light for 30 min in 0.8 M Tris (tris-hydroxymethyl-aminomethane) buffer at pH 8.5 and the suspension was centrifuged for 20 min at 35000*g* (the process denoted as Tris treatment). The Tris-treated PS II membranes were suspended in a solution of 0.2 M of sucrose, 20 mM of NaCl and Mes/NaOH (pH 6.8 at 20°C) containing 50% glycerol (w/v), stored in liquid N_2, and used for determination of the distance between $Y_D^{\bullet}$ and Chl_Z^+. To prepare the oriented samples, the PS II membranes were dried on mylar sheets under N_2 atmosphere with 90% humidity at 4°C for 16 h [27]. The sheets were cut into strips of 3 by 20 mm^2 and transferred into Suprasil quartz tube of 4 mm inner diameter (a stack of five strips per sample tube). The sample tube was filled with He gas, sealed and stored in liquid nitrogen until use. Before ESE experiments, the Mn-depleted sample was illuminated for 10 min at 200 K by a 500 W tungsten-halogen lamp through a 10 cm thick water filter. Immediately after illumination the sample was put into liquid nitrogen in order to trap Chl_Z^+ radical [29].

2.2 Measurements

The "2+1" ESE experiments have been performed on a pulsed EPR spectrometer ESP380 (Bruker) with a pulse sequence shown in Fig. 1. The spectrometer was equipped with a cylindrical dielectric cavity (ER4117DHQ-H, Bruker) and a nitrogen gas flow system (CF935, Oxford Instruments). The measurement temperature was about 80 K and microwave pulses (mw) of 16, 24 and 16 ns du-

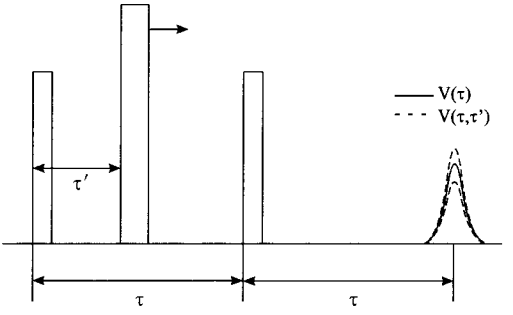

Fig. 1. The pulse sequence of the "2+1" ESE method. The primary ESE signal is formed by the first and third mw pulses with a carrier frequency ω, separated by the time interval τ. The amplitude of the ESE signal is observed as a function of the position τ' of the second mw pulse with the same carrier frequency. The mw field amplitude, H_1, in three pulses was set to provide the spin rotation angles 30, 60, and 30°, respectively.

rations were used. The mw magnetic field amplitude, H_1, in the three pulses was set to provide the spin rotation angles of 30, 60, and 30°, respectively.

The continuous-wave (cw) EPR measurement was performed on a Varian E-109 X-band EPR spectrometer at 77 K with a finger-type dewar inserted in a TE_{102} rectangular cavity to observe signals in the trapped state. EPR of Cr^{3+}-doped MgO (g = 1.9800) attached on the cavity wall was used for references of g-values, signal intensities and mw powers.

3 Theory

The principles of "2+1" ESE method, a special case of general ELDOR (electron-electron double resonance) method [19, 20], have already been discussed in the original works [19–22] and in our previous works on PS II [23, 25, 28] and will not be reiterated here. The pulse sequence is given in Fig. 1. In the "2+1" method the mw frequencies of three pulses are the same. Accordingly, the "2+1" method is used to determine the dipole interaction between the spins with overlapping EPR spectra.

For pairwise distributed spins, the primary ESE signal intensity in the "2+1" method depends on the time position of the second mw pulse, τ', as described by the following formula [21–25, 28]:

$$V(\tau,\tau') \propto 1 - 2\langle S_3\rangle \sin^2(\pi D\tau) - 2\langle S_2\rangle \sin^2(\pi D\tau') + \langle S_2 S_3\rangle\left[\sin^2(\pi D\tau') - \sin^2\left(\pi D(\tau-\tau')\right) + \sin^2(\pi D\tau)\right] . \quad (1)$$

In this expression D is the secular component of the dipole interaction between the radical spins

$$D = D_0(1 - 3\cos^2\theta_R) \quad (2)$$

with θ_R being the angle between the static magnetic field $\mathbf{B}_0$ and the distance vector $\mathbf{R}$ joining the spins in the pair. The dipole interaction constant D_0 is directly related to the distance between the spins

$$D = (g\beta)^2/hR^3 . \quad (3)$$

The EPR spectra of the paired spins in Eq. (1) are assumed to have similar g-factors and line shapes. Besides, these spectra should be narrow enough to provide for the efficient excitation of both spins by the mw pulses with a single carrier frequency and typical $B_1 \sim 1$ mT. It has been noted that for the spectra of $Y_D^{\bullet}$ and Chl_Z^{+} these two conditions are satisfied.

In a disordered system the dependence given by Eq. (1) is to be averaged over all possible orientations of the distance vector $\mathbf{R}$ with respect to the laboratory frame

$$\langle V(\tau,\tau')\rangle_{dis} \propto \int_0^{\pi} V(\tau,\tau')\sin\theta_R \, d\theta_R , \quad (4)$$

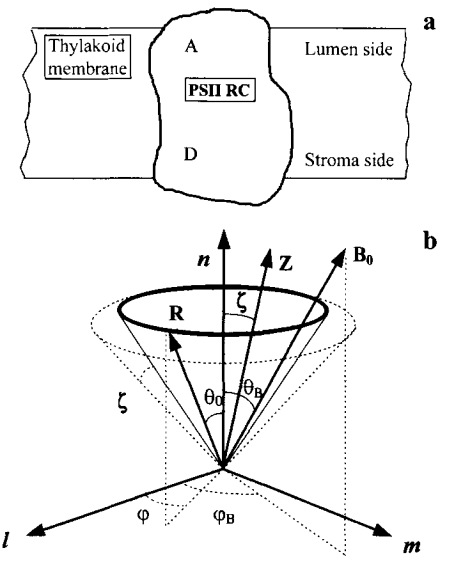

Fig. 2. **a** Schematic drawing showing PS II RC in a fragment of a thylakoid membrane; D and A designate the donor and the acceptor side of the PS II RC. **b** Orientation of a PS II RC and the magnetic field $\mathbf{B}_0$ with respect to the membrane coordinate system (**l**, **m**, **n**), where **n** is a membrane normal while **l** and **m** are arbitrary orthogonal axes in the membrane plane. Axis **Z** is associated with the PS II RC (see **a**), whose deviation from **n**-axis is defined by ζ. We can always choose **l** and **m** in such a way that **Z** is perpendicular to the (**l**, **m**) plane. All orientations obtained by a rotation of the PS II RC around **Z** by an arbitrary angle φ are assumed to have equal probability.

where the subscript "dis" stands for disordered sample. The resulting dependences will show damping oscillations with a frequency close to that realized in a statistically most probable orientation with $\theta_B = 90°$. For pertinent examples one can refer to our previous studies, where the distance between $Y_D^{\bullet}$ and Chl_Z^{+} has been determined to be 29.4 ± 0.5 Å.

In an oriented system, however, the orientational averaging is different from Eq. (4). The PS II RC is in the thylakoid membranes in such a way that the donor and acceptor sides of PS II are situated at opposite sides of the membrane. A schematic representation is shown in Fig. 2a. We may associate with the PS II RC a coordinate frame (X, Y, Z). Axis Z of this frame is shown in Fig. 2b. The angle between this axis and the membrane normal **n** is denoted by ζ. This angle may vary within some limits, but we can always choose the (X, Y, Z) system in such a way that $\zeta = 0$ will represent a center of the ζ distribution.

We will allow for the random deviation of the PS II RC orientation angle ζ with respect to **n** (see Fig. 2b) in the range from 0 to ζ_0. All the orientations obtained by the rotation of PS II RC around axis Z by an arbitrary angle ζ will be assumed to have equal probability. Angle θ_R between **R** and $\mathbf{B}_0$ is then expressed as

$$\begin{aligned}\cos\theta_R = {} & \cos\theta_B(\cos\zeta\cos\theta_0 - \sin\zeta\sin\theta_0\cos\varphi) \\ & + \sin\theta_B\cos\varphi_B(\sin\zeta\cos\theta_0 + \cos\zeta\sin\theta_0\cos\varphi) \\ & + \sin\theta_B\sin\varphi_B\sin\theta_0\sin\varphi \ , \end{aligned} \tag{5}$$

where θ_0 is the angle between **n** and **R**, the one to be determined in the experiment, θ_B is the angle between $\mathbf{B}_0$ and **n** and φ_B is the angle describing a rotation of $\mathbf{B}_0$ around **n** (see Fig. 2b).

Actually the deviation from the average orientation of the membrane normal should be taken into consideration as a Gaussian distribution $G(\delta)$, that is converted to the distribution of magnetic field orientation $\delta = \theta - \theta_B$. Averaging over the distribution of orientation is given by

$$\langle V(\tau,\tau')\rangle_{\text{ori}} \propto \int_0^{\pi}\int_0^{2\pi}\int_0^{2\pi}\langle V(\tau,\tau')\rangle \mathrm{d}\varphi_B \mathrm{d}\varphi G(\theta-\theta_B)\sin\theta \mathrm{d}\theta \ , \tag{6}$$

where $G(\delta) = N\exp(-\zeta^2/\zeta_0^2)$ with $\zeta = \theta - \theta_B$ and ζ_0 is a root mean square deviation and N is a normalization factor. The value of θ_0 will be determined by simulation of Eq. (6) for the fixed value of D_0 and θ_B for the magnetic field orientation by assuming a trial value of ζ_0.

4 Results

The cw EPR spectra of Y_D radical in Mn-depleted PS II for membrane-oriented preparation were observed at θ_B = 90, 60, 30, and 0° at 80 K as shown in Fig. 3. From the variations seen in the angular dependence one can conclude that the samples are indeed partially oriented.

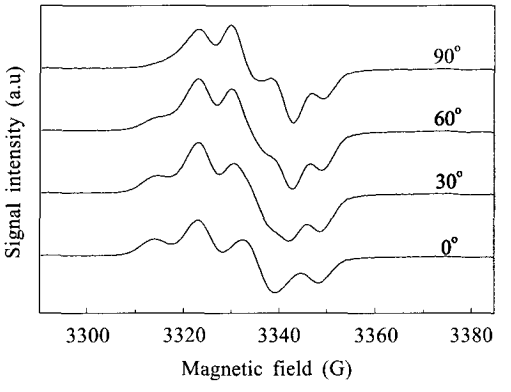

Fig. 3. Cw EPR signals of $Y_D^{\cdot}$ in Mn-depleted PS II at the angles θ_B of 90, 60, 30, and 0° of partially oriented membranes observed after dark adaptation. EPR conditions: mw frequency, 9.34 GHz; mw power, 0.25 μW; field modulation frequency, 100 kHz; field modulation amplitude, 3.2 G.

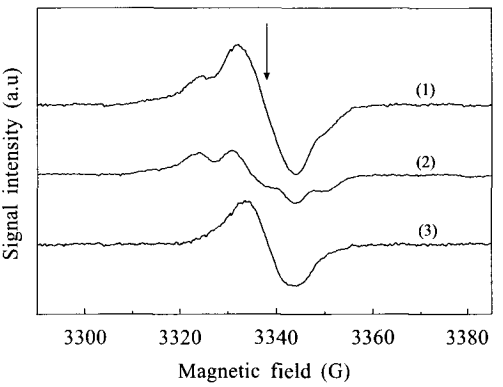

Fig. 4. Cw EPR signals of $Y_D^{\bullet}$ and Chl_Z^+ in the Mn-depleted PS II membranes observed at 77 K for $\theta_B = 90°$. Trace 1: Overlapped EPR spectra of $Y_D^{\bullet}$ and Chl_Z^+, trapped by freezing into 77 K after illumination at 200 K for 10 min. The arrow shows the position of $g = 2.0024$, where "2+1" ESE traces were observed. Trace 2: cw EPR spectra of $Y_D^{\bullet}$, observed after the dark adaptation of the same sample for 30 min at 273 K. Trace 3: cw EPR spectrum of Chl_Z^+ obtained by subtraction of trace 2 from trace 1. EPR conditions: mw frequency, 9.34 GHz; mw power 0.25 μW; field modulation frequency, 100 kHz; field modulation amplitude, 3.2 G.

In Fig. 4, trace 1 shows the EPR spectra of overlapped $Y_D^{\bullet}$ and Chl_Z^+, trapped by illumination at 200 K for 10 min in Tris-treated PS II. As we illuminated the samples at 200 K, most of the induced radical signals can be assigned to Chl_Z^+ [29]. After the dark adaptation at 273 K for 30 min, only the $Y_D^{\bullet}$ EPR signal remained as shown in trace 2. The Chl_Z^+ EPR signal was obtained by subtraction of $Y_D^{\bullet}$ EPR signal trace 2 from the overlapped EPR signal of $Y_D^{\bullet}$ and Chl_Z^+ trace 1 and is shown as trace 3. The intensity of Chl_Z^+ obtained by double integration on trace 3 was about 70% of that of $Y_D^{\bullet}$ in trace 1.

The "2+1" ESE experiment was performed at a fixed value of $\tau = 1200$ ns, with τ' varying from 80 to 1184 ns, where the magnetic field was fixed at the center of EPR spectrum indicated by the arrow in Fig. 4, trace 1. The angular dependence of the primary ESE amplitude on τ', measured in the membrane-oriented sample with trapped $Y_D^{\bullet}Chl_Z^+$ radical pair, is shown in Fig. 5. Trace 1 in Fig. 5 was recorded for dark-adapted Mn-depleted PS II particles with the orientation $\theta_B = 90°$ that shows $Y_D^{\bullet}$ signal only. It does not show any oscillation due to the dipole interaction between $Y_D^{\bullet}Chl_Z^+$ radical pair. As the concentration of reaction centers is very low (less than 50 μM RC with average separation of more than 150 Å between Y_D radicals), there is no detectable dipole interaction between Y_D radicals, and the experimental "2+1" trace shows no oscillatory behavior. Furthermore a statistical distribution over the wide range of distances produces only an exponential decay with no oscillatory behavior. The "2+1" ESE traces recorded for the illuminated Mn-depleted PS II at the orientations with $\theta_B = 90$, 60, 30, and 0° are shown by open circles in Fig. 5, trace 2. The τ' dependence reveals about two periods of low-frequency oscillation of about 2 MHz, which differs remarkably from that in trace 1 obtained in the dark-adapted sample where only Y_D radicals survive. Therefore, in the illuminated sample, the

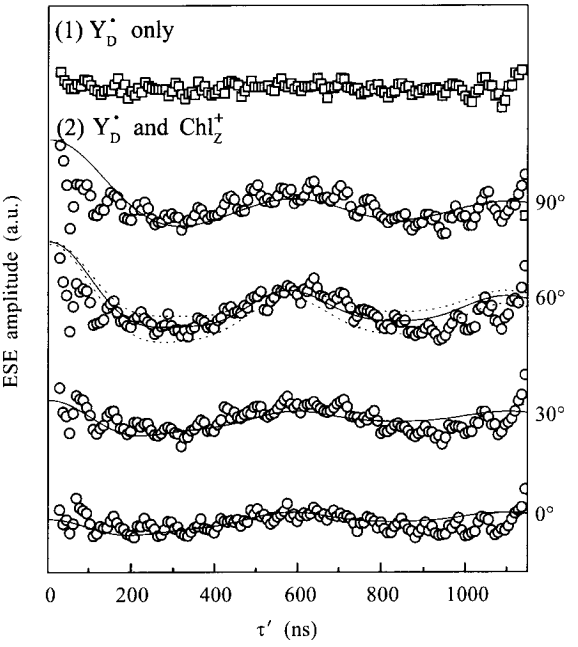

Fig. 5. "2+1" ESE traces recorded in the Mn-depleted PS II membranes for the orientations with θ_B = 90, 60, 30, and 0°. Trace 1 shows the time profile observed in the dark-adapted ($Y_D^{\bullet}$) for θ_B = 90° and traces 2 show the profiles in the illuminated ($Y_D^{\bullet}$ and Chl_Z^{+}) sample, for 90, 60, 30, and 0°. $Y_D^{\bullet}$ and Chl_Z^{+} radicals were trapped by illumination at 200 K for 10 min. EPR conditions: temperature, 80 K; τ = 1200 ns; magnetic field, 3450 G; mw frequency, 9.61 GHz. Solid lines, calculated for the dipole interaction constant D_0 = 2 MHz and the angle θ_0 = 50.0°, between **R** and the **n**-axis. The broken lines on the time profile for θ_B = 60° are drawn with the value θ_0 = 45.0 and 55.0°, to show the error range of ±5°. Deviation of the membrane normal from the average orientation is taken into consideration as a Gaussian distribution function of ζ ($=\theta - \theta_B$) with the value of ζ_0 = 15° (see text).

observed oscillating time profiles can be indeed ascribed to the dipole interaction between $Y_D^{\bullet}$ and Chl_Z^{+}.

It has already been shown [30] that this low-frequency oscillation originates from the dipole interaction in the pair formed by $Y_D^{\bullet}$ and Chl_Z^{+} in the same reaction center of the illuminated sample of nonoriented Mn-depleted PS II membranes. For the $Y_D^{\bullet}$ and Chl_Z^{+} pair, the value of the dipole interaction constant D_0 was determined to be 2.05 ± 0.1 MHz [30]. From this value of D_0, the distance between $Y_D^{\bullet}$ and Chl_Z^{+} was estimated to be 29.4 ± 0.5 Å. In this work, with the value of $D_0 \approx 2.0$ MHz and the simulations of Eq. (6) in theory over various angles of θ_0 to find the best fit for the field directions θ_B = 90, 60, 30, and 0°, the angle between the distance vector from Y_D to Chl_Z, **R**, and the membrane normal, **n**, is estimated to be 50.0 ± 5°. For the deviation of orientation from the average normal, a Gaussian distribution function of ζ ($=\theta - \theta_B$) as given by $1/\sqrt{2\pi\zeta_0^2}\exp[(-1/2)\zeta^2/\zeta_0^2]$ is taken into consideration, where ζ_0^2 is a mean square deviation of the value of $(15°)^2$. This value was usually deter-

mined by angular variation of fitting so that the angular variation will fit all the angles. However the value of 15° has usually been used in every case of oriented membranes in our laboratory, which includes statistical distribution of membrane orientation and the misalignment of the magnetic field directions relative to the direction of the average membrane normal. Solid lines in Fig. 5 show the successful fits with the experimental profiles for the $D_0 = 2.0$ MHz and the angle of $\theta = 50°$. The error range of $\pm 5°$ is shown only for 60°, where most pronounced effects will be expected to be seen for the direction of the distance vector nearly parallel to the magnetic field.

5 Discussion

In our recent works, distances and angles of several radical pairs were determined in PS II with pulsed EPR methods. They are 39 Å and 13° for Y_D-Q_A pair [31], 29 Å and 100° for Y_D-Y_Z, 27 Å and 110° for Y_D-Mn (the S_2-state multiline) [28] as determined by ELDOR method. 27 Å and 21° for P680-Q_A were determined by means of spin polarized radical pair ESEEM [32]. The accuracies in distances are within 0.5–1 Å, while those in angles are in 4–5°. Because of difficulty of X-ray analysis, these data are useful to know the three-dimensional (3-D) structure of the electron transfer chain in the plant PS II. We tried to derive the 3-D arrangement of electron transfer components in PS II, using the data on Y_D-Q_A, Q_A-P680 and Y_Z-Y_D [31]. The distances between P680-Y_D or -Y_Z and their orientations relative to the membrane normal have been derived to be approximately 20 Å and 42°, respectively.

The values obtained by a "2+1" ESE method are most accurate among the values derived by other EPR methods, because other methods cannot detect selectively the magnetic dipole interaction between radicals in the form of oscillation frequency [33, 34]. With this method, the distance between $Y_D^{\bullet}$ and Chl_Z^{+} was estimated to be 29.4 ± 0.5 Å [30] and the angular dependence suggests that the angle between the distance vector from Y_D to Chl_Z, **R**, and the membrane normal, **n**, is 50.0 ± 5° in this work.

The purified reaction center which consists of the D1, D2 and cyt b_{559} proteins contains only 6 Chls [2–6]. By analogy to the bacterial photosynthetic reaction center (bRC), two of these Chls are thought to make up a "special-pair" P680, while two others are expected to be nearby monomeric Chls. Two remaining Chls are suggested to be redox-active Chl, Chl_Z, which is ligated to a histidine at position D1-117 and the other is redox-inactive Chl, so-called, "Chl_D" ligated to the histidine at position D2-117 [7]. Furthermore, the Chl_Z and Chl_D terminology reflects the 2-fold structural symmetry of PS II which is observed for the redox-active tyrosines, Y_Z and Y_D.

The location of Chl_Z in PS II was estimated to be 27 Å from the inner and the outer thylakoid surface and 39.5 ± 2.5 Å from the nonheme Fe(II) by the EPR measurement of the spin-lattice relaxation time [34]. In addition to these data, our present data will give new useful information to know the structure of PS II. If trapping the Chl^{+}-Q_A^{-} radical pair is possible, the position of Chl_Z will

be derived in 3-D. It will be necessary to know the distance between P680 and Chl_Z to understand the electron transfer side chain. At present the determination of the 3-D arrangement of electron transfer components are underway by detecting any trapped radical pair one by one.

Acknowledgements

The authors are indebted to Professor Tsvetkov for his motivation to apply the PELDOR method to photosystems. A.K. was supported by the Hyogo Science and Technology Association.

References

1. Miller A.-F., Brudvig G.W.: Biochim. Biophys. Acta **1056**, 1 (1991)
2. Gounaris K., Chapman D.J., Barber J.: FEBS Lett. **365**, 88–92 (1990)
3. Kobayashi M., Maeda H., Satoh K.: FEBS Lett. **260**, 138–140 (1990)
4. Montoya G., Yruela I., Picorel R.: FEBS Lett. **283**, 255–258 (1991)
5. Oren-Shamir M., Sai P.S.M., Scherz A.: Biochemistry **34**, 5523–5526 (1995)
6. Setlikova E., Ritter S., Setlik I.: Photosynth. Res. **43**, 201–221 (1995)
7. Stewart D.H., Cua A., Brudvig G.W.: Biochemistry **37**, 10040–10046 (1998)
8. Debus R.J.: Biochim. Biophys. Acta **1102**, 269–352 (1992)
9. Miller A.-F., Brudvig G.W.: Biochim. Biophys. Acta **1056**, 1–18 (1991)
10. Svensson B., Styring S.: EMBO J. **7**, 2051–2059 (1990)
11. Ruffle S.V., Donnelly D.A., Nugent J.H.: Photosynth. Res. **34**, 287–300 (1992)
12. Thompson L.K., Brudvig G.W.: Biochemistry **27**, 6653–6658 (1988)
13. de Paula J.C., Innes J.B., Brudvig G.W.: Biochemistry **24**, 8114–8120 (1985)
14. Allakhverdiev S.I., Klimov V.V., Carpentier R.: Biochemistry **36**, 4149–4154 (1997)
15. Barber J., De Las Rivas J.: Proc. Natl. Acad. Sci. USA **90**, 10942–10946 (1993)
16. Nedbal L., Samson G., Whitmarsh J.: Proc. Natl. Acad. Sci. USA **89**, 7929–7933 (1992)
17. Buser C.A., Diner B.A., Brudvig G.W.: Biochemistry **31**, 11449–11459 (1992)
18. Poulson M., Samson G., Whitmarsh J.: Biochemistry **34**, 10932–10938 (1995)
19. Moliv A.D., Salikhov K.M., Shirov M.D.: Fiz. Tverd. Tela **23**, 975 (1981)
20. Milov A.D., Ponomarev A.B., Tsvetkov Yu.D.: Chem. Phys. Lett. **110**, 67 (1984)
21. Kurshev V.V., Raitsimring A.M., Tsvetkov Yu.D.: J. Magn. Reson. **81**, 441 (1989)
22. Kurshev V.V., Raitsimring A.M., Ichikawa T.: J. Phys. Chem. **95**, 3564 (1991)
23. Astashkin A.V., Kodera Y., Kawamori A.: Biochim. Biophys. Acta **1187**, 89 (1994)
24. Kodera Y., Hara H., Astashkin A.V., Kawamori A., Ono T.-A.: Biochim. Biophys. Acta **1232**, 43 (1995)
25. Hara H., Kawamori A., Astashkin A.V., Ono T.-A.: Biochim. Biophys. Acta **1276**, 140 (1996)
26. Kuwabara T., Murata N.: Plant Cell Physiol. **23**, 533–5399 (1982)
27. Rutherford A.W.: Biochim. Biophys. Acta **807**, 189 (1985)
28. Astashkin A.V., Hara H., Kawamori A.: J. Chem. Phys. **108**, 3805–3812 (1998)
29. Noguchi T., Mitsuoka T., Inoue Y.: FEBS Lett. **356**, 179–182 (1994)
30. Shigemori K., Hara H., Kawamori A., Akabori K.: Biochim. Biophys. Acta **1363**, 187–198 (1998)
31. Yoshii T., Kawamori A., Tonaka M., Akabori K.: Biochim. Biophys. Acta **1413**, 43–49 (1999)
32. Yoshii T., Kawamori A., Akabori K., Iwaki M., Itoh S.: Appl. Magn. Reson. **16**, 565–580 (1999)
33. Kodera Y., Hara H., Astashkin A.V., Kawamori A., Ono T.-A.: Biochim. Biophys. Acta **1232**, 45 (1995)
34. Koulougliotis D., Innes J.B., Brudvig G.W.: Biochemistry **33**, 11814–11822 (1994)

Authors' address: Asako Kawamori, Faculty of Science, Kwansei Gakuin University, Uegahara 1-1-155, Nishinomiya 662-8501, Japan